In-Beam electron spectroscopy of ^{226}U and ^{254}No

R.D. Humphreys,[1] P.A. Butler,[1, *] J.E. Bastin,[1] P.T. Greenlees,[2] N.J. Hammond,[1, †]

R.-D. Herzberg,[1] D.G. Jenkins,[1, ‡] G.D. Jones,[1] H. Kankaanpää,[2] A. Keenan,[2] H.

Kettunen,[2] T. Page,[1] P. Rahkila,[2] C. Scholey,[1] J. Uusitalo,[2] N. Amzal,[1, §] P.M.T. Brew,[1]

K. Eskola,[3] J. Gerl,[4] K. Hauschild,[5] K. Helariutta,[6] F.-P. Heßberger,[4] A. Hürstel,[5]

P.M. Jones,[2] R. Julin,[2] S. Juutinen,[2] T.-L. Khoo,[7] W. Korten,[5] P. Kuusiniemi,[2] Y.

Le Coz,[5] M. Leino,[2] A.-P. Leppänen,[2] M. Muikku,[2] P. Nieminen,[2] S.W. Ødegård,[8]

J. Pakarinen,[2] P. Reiter,[9] G. Sletten,[10] Ch. Theisen,[5] and H.-J. Wollersheim[4]

[1]*Oliver Lodge Laboratory, University of Liverpool, Liverpool L69 7ZE, UK*

[2]*University of Jyväskylä, 40014 Jyväskylä, Finland*

[3]*Department of Physics, University of Helsinki, 00014 Helsinki, Finland*

[4]*GSI, 64291 Darmstadt, Germany*

[5]*DAPNIA/SPhN CEA-Saclay, F-91191 Gif-sur-Yvette, France*[¶]

[6]*Department of Chemistry, University of Helsinki, 00014 Helsinki, Finland*

[7]*Argonne National Laboratory, Illinois 60439, USA*

[8]*Department of Physics, University of Oslo, N-0316 Oslo, Norway*

[9]*Ludwig Maximilians Universität, D-85748, Garching, Germany*

[10]*Niels Bohr Institute, 2100 Copenhagen, Denmark*

(Dated: March 26, 2004)

Abstract

The energy of the $2^+ \rightarrow 0^+$ transition in ^{226}U has been measured as 81.3(6) keV and the energy of the $4^+ \rightarrow 2^+$ transition in ^{254}No has been measured as 101.1(6) keV, both for the first time, by means of electron spectroscopy. The results are close to the estimates of the energies of these transitions from earlier γ-decay work. Absolute values of electromagnetic decay intensities have been measured for yrast transitions in both nuclei.

[*]corresponding author

[†]present address: Argonne National Laboratory, Illinois 60439, USA

[‡]present address: Nuclear Physics Group, Dept. of Physics, University of York, Heslington, YO10 5DD, UK

[§]present address: Department of Physics, University of Paisley, Paisley PA1 2BE

[¶]present address: CSNSM, bat. 104-108, 91405 Orsay Campus, France

I. INTRODUCTION

The study of the structure of the heaviest elements is important in order to understand the properties of the mean field when extrapolated far beyond the region of stability [1, 2]. While the observation of spherical superheavy nuclei has proved elusive so far, the study of the structure of deformed nuclei in the middle of this "superheavy" shell can also reveal much about the parameterisation of the mean field. For example the rotational behaviour of ^{254}No [3–5] and ^{252}No [6] up to spin 20 $\hbar$ has been studied using γ-ray spectroscopy, in which γ-ray transitions were identified using recoil and α-decay tagging techniques. (For a recent review see Herzberg [7].) However, for the heaviest nuclei the sensitivity of γ-ray spectroscopy is reduced by the presence of internal conversion. The probability that an excited nucleus decays via internal conversion increases with increasing Z number and with decreasing transition energy. For these reasons the observation of low energy transitions in the heaviest elements is not possible using germanium detector arrays. This makes it difficult to study odd mass nuclei and $K \neq 0$ rotational bands in even-even nuclei where the probability of $M1$ decay becomes large compared to other electromagnetic modes. For the ground state rotational bands of well deformed even-even nuclei the transition energies between the lowest states cannot be measured using γ-ray spectroscopy and have been deduced by extrapolation from a Harris fit to the higher spin transitions. It is therefore important to measure the lower energy transitions where possible.

The electron spectrometer SACRED [8] was designed to overcome these problems in studying the heaviest nuclei and also to reveal information additional to that obtained from γ-ray spectroscopy. The spectrometer allows the simultaneous direct detection of multiple conversion electrons emitted at the target, with high efficiency. It is coupled to the gas filled recoil separator RITU [9] so that weakly populated nuclei can be studied effectively. This paper describes how the SACRED spectrometer was used to measure the low-lying transitions of the ground state bands in ^{226}U and ^{254}No.

II. EXPERIMENTAL DETAILS

A. SACRED spectrometer

The following is a brief description of the construction and operation of the SACRED spectrometer, which will be described in more detail in a forthcoming publication [10]. The SACRED spectrometer consists of a Si PIN wafer, 500 microns thick, divided into 25 elements, each connected to an individual DC coupled preamplifier. The elements are arranged in a circular geometry, consisting of six quadranted annuli surrounding a central element. The diameter of the detector is 27.6 mm. The detector and first stage amplification are mounted on a PCB inside the detector vacuum housing. In order to improve its energy resolution the detector is cooled to a temperature of approximately -20C by radiation to a black copper plate in thermal contact with a liquid nitrogen bath.

Electrons are transported from the target to the detector by four normal conducting magnetic coils, which are capable of producing a solenoidal field of $\approx$0.3 T when at an operating current of 560 A. A profile of the magnetic field along the solenoid axis is given in figure 1. The solenoid axis is positioned at an angle of 177.5° with respect to the beam axis, the beam passing through a hole 12 mm in diameter at a distance of 25 mm from the centre of the detector and in the same plane, creating an approximately collinear geometry. A true collinear geometry would require an annulus at the centre of the detector, significantly reducing the detection efficiency for low energy electrons. The approximate collinear geometry offers the advantages of reducing both Doppler line shape broadening and delta electron flux at the detector. Most of the flux of low energy electrons is suppressed by an electrostatic barrier situated between the target and detector.

The greatest benefit of the near collinear geometry is that it enables SACRED to be used in conjunction with the gas filled recoil separator RITU. Fusion-evaporation residues are magnetically separated from unwanted products, and transported to a 16 strip silicon detector situated at the focal plane of RITU. The helium gas used in RITU and the target section of SACRED is separated from the rest of SACRED by an assembly of two 60 μg/cm^2 carbon foils with pumped intermediate volume [10]. The use of two foils allows the pressure in the volume containing the electrostatic barrier to be maintained at $\approx 10^{-6}$ torr. Low pressure in the barrier and detector region is necessary in order to reduce the background
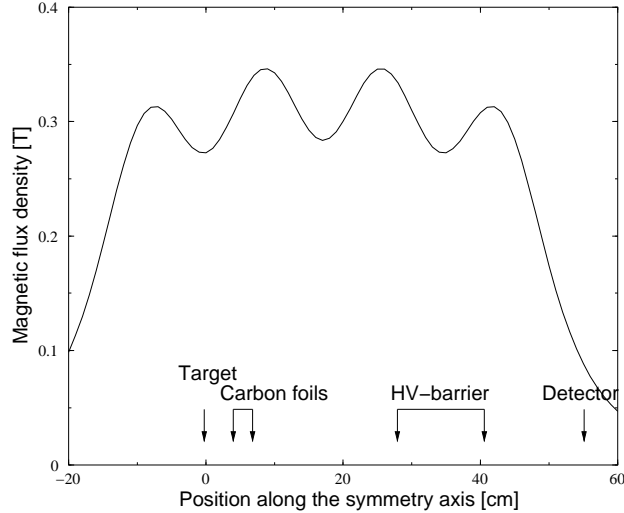
3

FIG. 1: Calculated magnetic field profile along the solenoid axis for current I = 560 A.

from accelerated electrons, produced when residual gas molecules in the region between the barrier and detector are ionised by the beam.

In order to minimise dead-time and pile-up the counting rates of the individual detector pixels were maintained at less than 12 kHz. A number of measures are taken to ensure that the flux of electrons having a wide range of energies is evenly distributed over all the pixels. Firstly, the detector is placed in a region of low magnetic flux density (see figure 1), secondly, the beam is deliberately defocused at the target and finally, the geometry of the detector is such that the area of the pixels increases towards the outer segments. The positioning of the detector in a region of low magnetic flux density also reduces the probability of electrons backscattering from the surface of the detector [8].

B. Description of experiments

An example of the absolute efficiency curve can be seen in figure 2 [10], measured for a barrier potential of -40kV. The figure also shows the simulated response, calculated in the manner described by Butler et al. [8] that takes into account multiple scattering in the detector. The simulation is in good agreement with the data for electron energies < 300keV.

Two experiments were carried out at the Accelerator Laboratory of the University of Jyväskylä. In the first experiment a beam of 112 MeV ^{22}Ne, with an average intensity of 8.5 particle nA, irradiated a ^{208}Pb target, of 200 μg/cm^2 thickness, for approximately 29
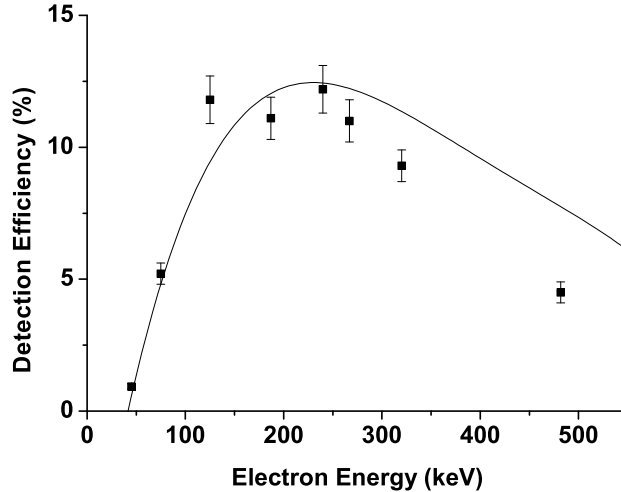
4

FIG. 2: Absolute efficiency curve for the SACRED spectrometer obtained using a ^{133}Ba electron source. The electrostatic barrier in this case was -40 kV. The solid line is from simulations using the SOLENOID Monte Carlo code [8].

hours, with a helium gas pressure of 0.3 mbar in the magnetic volume of RITU and the target section of SACRED. Under these conditions the counting rate in the centre pixel of the detector, where the rate is highest, is about 12 kHz. The rates in the pixels drop rapidly with radius from the centre, to around 8 kHz half way across the detector and 2 kHz at the outermost pixel. The electrostatic barrier potential was -35 kV for this experiment. The maximum cross-section for the reaction ^{208}Pb(^{22}Ne,4n)^{226}U is approximately 6 μb [11], compared to 300 μb for the dominant αxn channels leading to isotopes of Thorium. Although the efficiency of RITU for detection of the latter channel is much smaller than for the former, the use of some form of channel selection is necessary in order to retrieve events of interest. For the reaction used the uranium recoils are not energetic enough to allow the use of a parallel plate proportional counter, placed in front of the focal plane silicon detector, for heavy recoil identification. Channel selection in this case was achieved using the method of Recoil Decay Tagging (RDT) [12]. The recoils were identified by requiring that their subsequent α-decay corresponded to the ^{226}U α-decay energy (see figure 3), at the same position in the Si-strip detector, within a maximum time interval of 800 ms (approximately three half-lives of ^{226}U). Figure 3b shows α events which occurred up to 800 ms after the implantation of a recoiling nucleus. Only events in the energy range 7506-7608 keV were
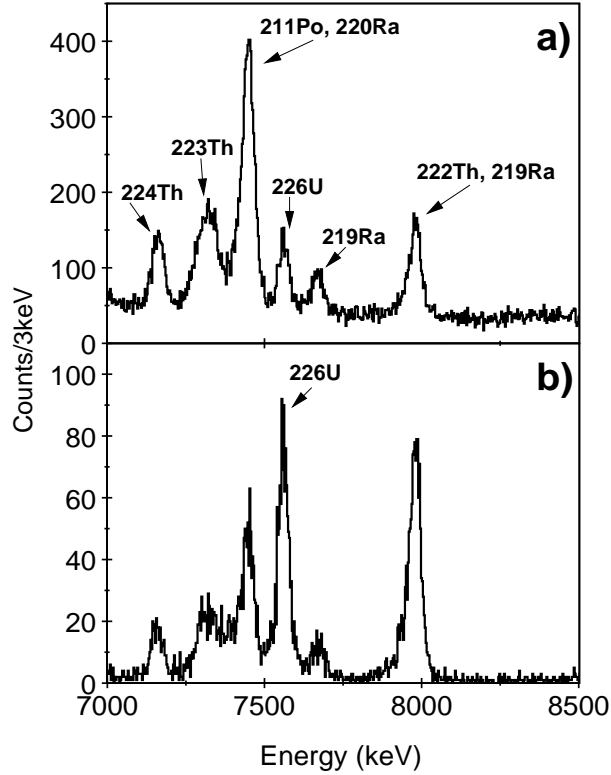
5

FIG. 3: (a) Focal plane spectrum of alpha particles expanded about the energy region of interest. (b) α events occurring within 800 ms of recoil implantation.

accepted as possible ^{226}U α-decays. Using this method 1230 recoils were tagged.

In the second experiment a beam of 219 MeV ^{48}Ca was used with an average estimated beam energy at the centre of the target of 216 MeV, corresponding to the maximum yield for ^{254}No. Two separate targets of 98% enriched ^{208}Pb were employed during the experiment. The first target, having thickness 400 μg/cm^2 was irradiated by a beam of 1.6 particle nA for approximately 106 hours. The second, having thickness 250 μg/cm^2, was irradiated by a beam of 3 particle nA for approximately 123 hours. The magnetic volume of RITU and the target section of SACRED were maintained at a helium gas pressure of 0.7 mbar for both experiments. In these experiments the electrostatic barrier was -40 kV. In the first run, 2440 recoils were detected and in the second 4710. Unlike the ^{226}U experiment there were no competing fusion reaction channels. The target purity of 98% ^{208}Pb ensures negligible competition from the reaction ^{207}Pb(^{48}Ca,2n)^{253}No [13], and the combined population of
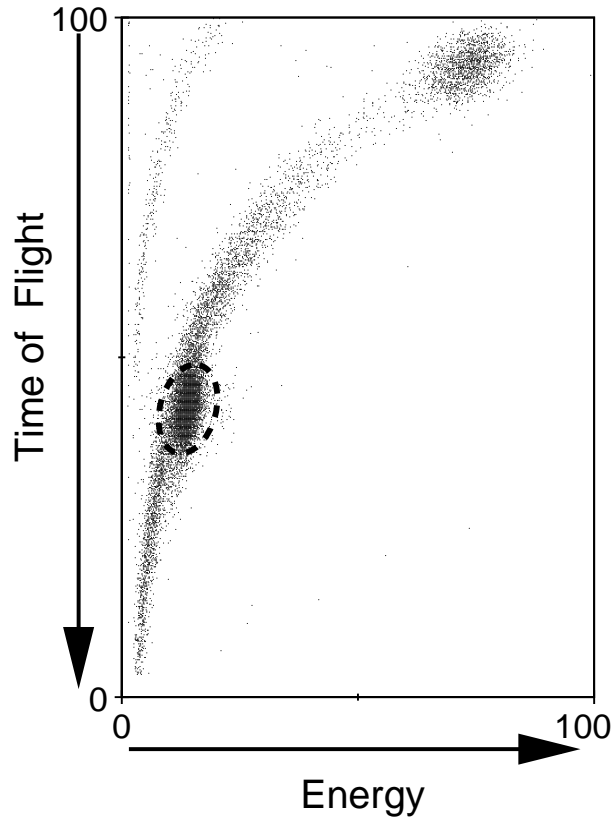
6

FIG. 4: Focal plane energy vs. Time of Flight with arbitrary units on both axes. The region bounded by the dashed line contains events corresponding to ^{254}No recoils.

^{253,255}No from the 3n and 1n channels is about 1% of that of ^{254}No [14, 15] making the use of the RDT technique unnecessary. For the reaction used in these experiments the nobelium recoils are sufficiently energetic to allow the use of a parallel plate proportional counter, placed in front of the silicon detector which allows the heavy recoils to be distinguished from unwanted products such as scattered beam, see figure 4. This procedure has been verified [16] using the RDT technique in which ^{254}No recoils were selected by gating on their subsequent alpha decays.
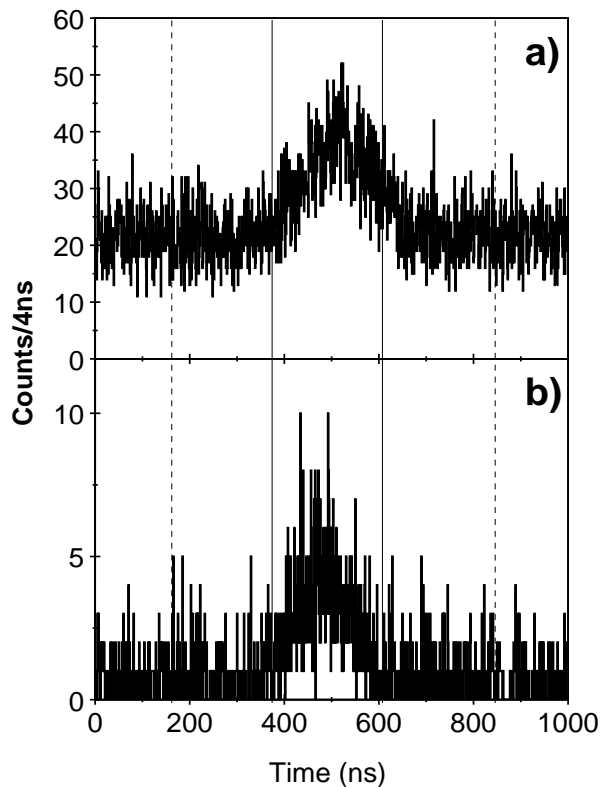
FIG. 5: (a) TDC started by a recoil event in the focal plane and stopped by the detection of an electron in the target position. (b) The same as (a) but in coincidence with recoils correlated to the decay of ^{226}U. The region between the solid lines represents the prompt TDC gate used in the experiment. The region between solid and dashed lines either side represents the gates used to create the background contribution.

III. RESULTS

A. ^{226}U

In order to construct the conversion electron spectrum corresponding to ^{226}U transitions alone, the contribution from random coincidences was determined. Figure 5 shows the time distribution of events between prompt electrons detected using SACRED and the detection of ^{226}U recoils in the focal plane of RITU, measured using a Time-to-Digital-Converter (TDC). The gates used to increment the random spectrum and the true (+ random) spectrum are
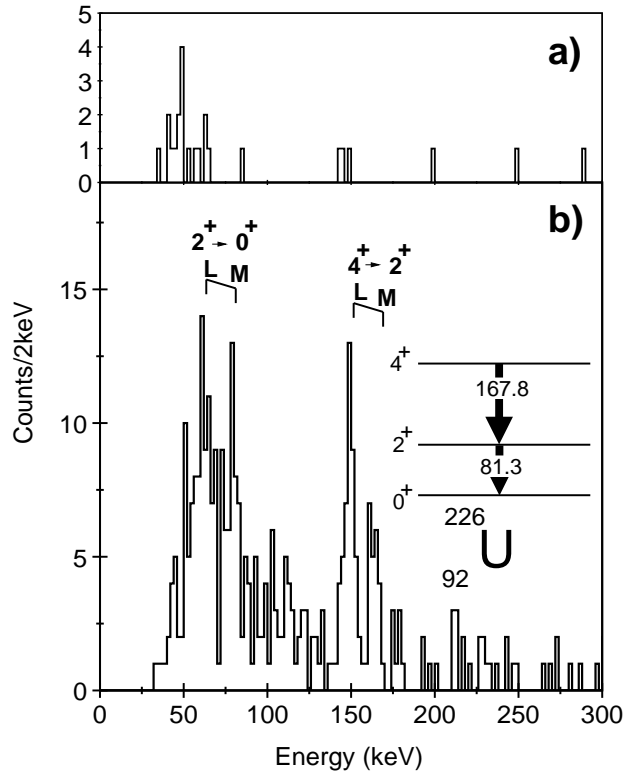
FIG. 6: (a) Normalised random background contribution for ^{226}U. (b) Experimental conversion electron spectrum in coincidence with recoils correlated to the decay of ^{226}U, corrected for the contribution from random coincidences.

shown in this figure. Figure 5a shows the total time distribution, and figure 5b shows the events corresponding to recoils identified as ^{226}U by their α-decay.

Figure 6a shows the normalised random background contribution used to correct the electron spectrum. Figure 6b shows the background corrected conversion electron spectrum of ^{226}U, in which the conversion electrons from the $2^+ \rightarrow 0^+$ and $4^+ \rightarrow 2^+$ transitions can be observed. The in-beam energy resolution of SACRED is typically 5-6 keV, insufficient to fully resolve the L_2 and L_3 subshell components (3.78 keV separation) and the various M subshells (< 1 keV separation). The efficiency of SACRED for the 81.3 keV L,M lines is reduced largely because of the effect of the electrostatic barrier. The collinear design of SACRED ensures that electrons emitted at angles to the beam direction of $> 130°$, with average angle of 150°, are accepted, thus reducing the Doppler broadening to < 2

9

TABLE I: Measured energies for ^{226}U. Column (a) lists the transition energies deduced here. Column (b) lists the transition energies estimated by Greenlees et $al.$ [18].

$I_i^{\pi i}$	$I_f^{\pi f}$	E_L	E_M	E_γ (a)	E_γ (b)
2^+	0^+	60.8(5)	78.2(7)	81.3(6)	80.5(5)
4^+	2^+	148.2(4)	162.51(6)	167.8(4)	168.7(6)

keV. Corrections to the electron energy arising from the Doppler shift of the electrons were calculated using the SOLENOID Monte Carlo code [8]. The code models the emission of electrons from the target and subsequent transportation to the detector. The average Doppler shift is calculated for many electron trajectories for a given input transition energy, using an iterative procedure. As an example of the magnitude of this effect, the Doppler shift of the 60.8 keV electron line in ^{226}U ($\beta \approx 0.0102$) was 2.3 keV, while for the 73.2 keV electron line in ^{254}No ($\beta \approx 0.0186$) the shift was 5.0 keV. Energy losses in the target are taken into account although losses in the carbon foils are ignored because the foils are also present when calibrating the detector with a ^{133}Ba source. In order to calculate the transition energy from the composite L and M peaks an average binding energy is needed. Using conversion coefficients from Rösel et $al.$ [17] the relative intensities of the L and M subshells were calculated and a weighted binding energy for the L and M atomic shells was determined for each observable energy transition. The weighted binding energy was then used in conjunction with the corrected electron energies to determine the energy of the given line. Table I shows the electron energy of the observed L and M lines, along with the derived transition energy, E_γ. The absolute intensities for transitions in ^{226}U are given in table II, calculated from the measured response curve for SACRED for an electrostatic barrier of -35 kV (c.f. fig. 2). The errors in the intensity values given in the table and in table IV do not include the $\approx 10\%$ systematic uncertainty coming from dead time in the data acquisition.

B. ^{254}No

An estimate of the random background contribution in ^{254}No was made in the same manner as discussed in the previous section, see figure 7 and figure 8a. Figure 8b shows the

TABLE II: Measured intensities for ^{226}U. In column (a) are the sum of the L and M electron counts experimentally observed. Column (b) gives the total transition intensities corrected using tabulated values of internal conversion coefficients [17] and the energy dependent absolute efficiency. Column (c) lists the total transition intensities per 1000 recoils. Column (d) lists the transition intensities taken from Greenlees *et al.* [18], normalised so that the intensity of the $4^+ \rightarrow 2^+$ transition has the same value as the absolute value measured in this experiment.

$I_i^{\pi i}$	$I_f^{\pi f}$	(a)	(b)	(c)	(d)
2^+	0^+	45(9)	870(220)	710(180)	660(200)
4^+	2^+	42(9)	630(130)	510(110)	510(80)

TABLE III: Measured energies for ^{254}No. Column (a) lists the transition energies deduced here. Column (b) lists the transition energies observed by Leino *et al.* [4]. Column (c) lists the transition energies observed by Reiter *et al.* [3]. The energies marked with an asterisk * represent Harris parameter predictions.

$I_i^{\pi i}$	$I_f^{\pi f}$	$E_{L_{1,2}}$	E_{L_3}	E_M	E_γ (a)	E_γ (b)	E_γ (c)
4^+	2^+	73.2(9)	78.6(9)	95(2)	101.1(6)	102*	102*
6^+	4^+	128.6(9)	136.4(9)	152(2)	157.7(6)	158.9(3)	159.1(3)
8^+	6^+	185.9(1.2)	192.6(1.2)	206(3)	214.2(8)	214.1 (3)	214.1(2)
10^+	8^+	237.8(1.4)	245.6(1.4)	258(4)	266.5(1.0)	267.2(3)	267.3(3)

recoil gated electron spectrum of ^{254}No in which transitions $10^+ \rightarrow 8^+$ down to $4^+ \rightarrow 2^+$ are labelled. Peaks which are not labelled are assumed to be from background events. The marked difference in background in this spectrum and in the ^{226}U spectrum was investigated in detail by Butler *et al.* [16]. That work concluded that the background was due to a large fraction of the entry states in ^{254}No decaying via M1 cascades, which arise from the population of rotational bands built upon high K-value bandheads. The same method for determining the transition energies was used for ^{254}No as for ^{226}U (see previous section). Table III shows the electron energy of the observed L and M lines, along with the derived transition energy E_γ. The energy of the $4^+ \rightarrow 2^+$ transition is in good agreement with the
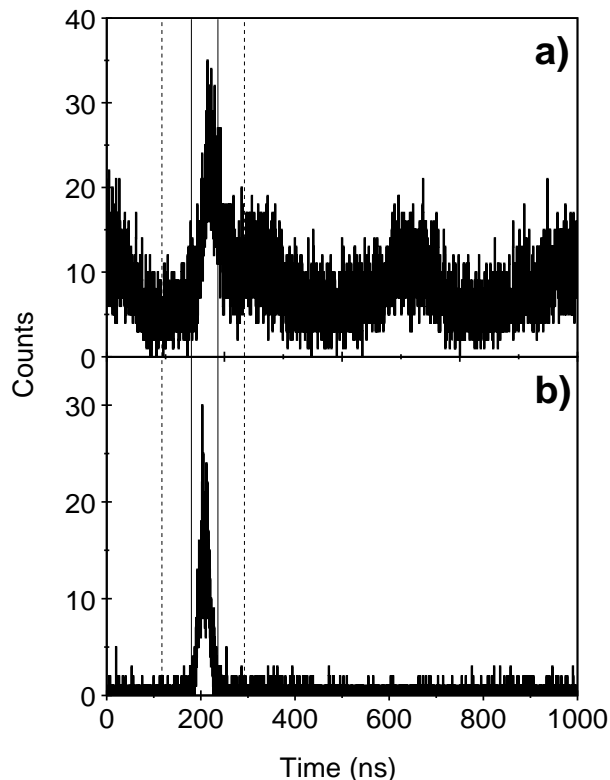
11

FIG. 7: (a) Time distribution, following the reaction ^{48}Ca + ^{208}Pb, between a recoil event in the focal plane in RITU and the detection of an electron in SACRED. (b) The same as (a) but for when the recoils were selected using the parallel plate gas detector. The region between the solid lines represents the prompt gate used in the experiment. The region between solid and dashed lines either side represents the gates used to create the background contribution.

value given in references [3],[4] which has been obtained using an extrapolation based on the Harris expansion. Unfortunately the $2^+ \rightarrow 0^+$ transition could not be observed because the expected electron energies are lower than the 40 keV threshold produced by the electrostatic barrier. The absolute transition intensities are also given in table IV. Relative values are compared to the intensities of the ground state band transitions obtained from γ-ray yields measured by Leino et al. [4]. It is observed that the population of the spin 4^+ state at 146 keV in ^{254}No (column (c)) is less than 50%. While not significantly smaller than for the 4^+ state at 250 keV in ^{226}U (see column (c) in table II), the low population in ^{254}No has been attributed to the presence of high K bands having isomeric band heads in this nucleus [16].
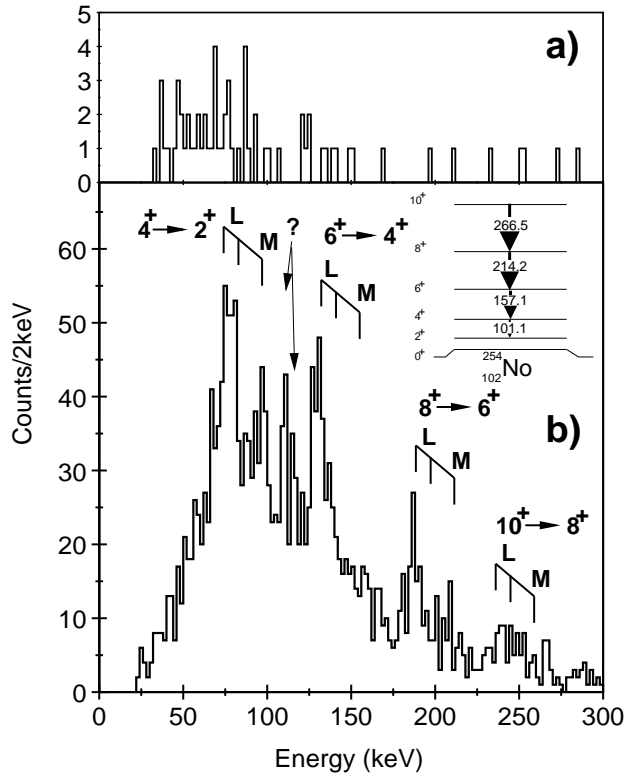
12

FIG. 8: (a) Normalised random background contribution for ^{254}No. (b) Experimental conversion electron energy spectrum in coincidence with ^{254}No recoils selected using the parallel plate gas detector. The unidentified peak is labelled as '?'.

Recoil-electron-electron coincident spectra are shown in figures 9(a)-(e)), in which the gates used to generate spectra in panels (b)-(e) include all L subshells. The coincidence data are consistent with the level scheme, although no additional information can be obtained due to the low statistics.

An unidentified peak having an energy of 112(1) keV was observed. The peak is within $\approx$ 6 keV of where the $10^+ \rightarrow 8^+$ K transition is expected. If the peak originated from the $10^+ \rightarrow 8^+$ K transition, an intensity of $\approx$ 16 counts would be expected, but the measured intensity (see table IV) is $\approx$ 70 and hence the origin of the major component lies elsewhere. It is possible that a component of this transition arises from a specific M1 transition in an high-K rotational band. Figure 9 suggests that the transition is in prompt ($<$ 50ns) coincidence with the $4^+ \rightarrow 2^+$ transition in the ground state band.

13

TABLE IV: Measured intensities for ^{254}No. The third column labelled (a) gives the sum of the L and M electron counts observed. Column (b) gives the electron intensities corrected for absolute efficiency and internal conversion [17]. Column (c) lists the total transition intensities per 1000 recoils. Column (d) lists the transition intensities taken from Leino *et al.* [4], normalised so that the intensity of the $6^+ \to 4^+$ transition has the same value as the absolute value measured in this experiment. The numbers marked with an asterisk * represent measurements made for the 112 keV peak uncorrected for internal conversion.

$I_i^{\pi i}$	$I_f^{\pi f}$	(a)	(b)	(c)	(d)
4^+	2^+	183(14)	3150(250)	440(35)	
6^+	4^+	175(15)	2180(190)	300(30)	300(100)
8^+	6^+	106(10)	1730(160)	240(20)	250(50)
10^+	8^+	54(7)	1280(170)	180(20)	220(40)
		70(8)*	780(90)*		

IV. CONCLUSION

An experimental technique has been developed for the detection of prompt conversion electrons emitted from weakly populated nuclei. In this way the $2^+ \to 0^+$ transition in ^{226}U and the $4^+ \to 2^+$ transition in ^{254}No have been identified for the first time. The absolute intensities for low-lying transitions in these nuclei have been measured for the first time. Electron-electron coincidences data have also been obtained that are consistent with the decay scheme. These data reveal that an identified 112 keV transition is in prompt coincidence with the lowest transitions in the ground state band.
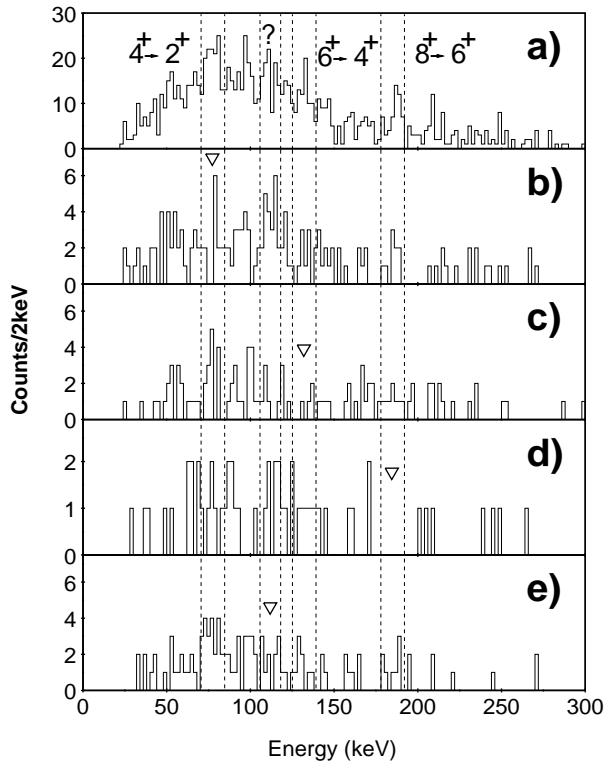
V. ACKNOWLEDGEMENTS

FIG. 9: Panels (a) to (e) are ^{254}No recoil tagged e-e coincidence spectra. Panel (a) shows the total projection of the coincident electron matrix. The dashed lines represent the gates set on the L electrons used to produce panels (b) to (e) in which the position of the gating transition is marked with a triangle: (b) electrons coincident with the $4^+ \rightarrow 2^+$ transition, (c) electrons coincident with the $6^+ \rightarrow 4^+$ transition; (d) electrons coincident with the $8^+ \rightarrow 6^+$ transition; (e) electrons coincident with the unidentified peak (labelled '?' in a)).

[1] S. Cwiok et al., Nucl. Phys. **A611**, 211 (1996)

[2] A.T. Kruppa et al., Phys. Rev. **C61**, 034313 (2000)

[3] P. Reiter et al., Phys. Rev. Lett. **82**, 509 (1999)

[4] M. Leino et al., Eur. Phys. J. A**6**, 63 (1999)

[5] P. Reiter et al., Phys. Rev. Lett. **84**, 3542 (2000)

[6] R.-D. Herzberg et al., Phys. Rev. C**65**, 014303 (2002)

[7] R.-D. Herzberg, J. Phys. G: Nucl. Part Phys. **30**, R123 (2004)

[8] P.A. Butler et al., Nucl. Instr. Meth. A**381**, 433 (1996)

[9] M. Leino et al., Nucl. Instr. Meth. B**99**, 653 (1995)

[10] H. Kankaanpää et al., to be published

[11] A.V. Yeremin et al., Nucl. Instr. Meth. A**350**, 608 (1994)

[12] K.H. Schmidt et al., Nucl. Phys. A**318**, 253 (1979)

[13] Yu. Ts. Oganessian et al., Phys. Rev. C**64**, 054606 (2001)

[14] M. Itkis et al., Nouv. Cim. **111**A, 783 (1998)

[15] V.J. Zagrebaev et al., Phys. Rev. C**65** 014607 (2001)

[16] P.A. Butler et al., Phys. Rev. Lett. **89**, 202501 (2002)

[17] F. Rösel et al., At. Data Nucl. Data Tables **21**, 91 (1978)

[18] P.T. Greenlees et al., J. Phys. G: Nucl. Part. Phys. **24**, L63 (1998)